doi: 10.4149/gpb_2018011

Rat liver intoxication with CCl_4: biochemistry, histology, and mass spectrometry

Olga Otrubova[1*], Monika Jerigova[2,3*], Sona Halaszova[4], Ladislav Turecky[5], Jana Muchova[5] and Dusan Velic[2,3]

[1] *Department of Occupational Medicine and Toxicology, National Toxicological Information Centre, University Hospital Bratislava, Faculty of Medicine, Comenius University, Limbova 5, 833 05, Bratislava, Slovakia*
[2] *International Laser Center, Ilkovicova 3, 841 04 Bratislava, Slovakia*
[3] *Department of Physical and Theoretical Chemistry, Faculty of Natural Sciences, Comenius University, Ilkovicova 6, 842 15 Bratislava, Slovakia*
[4] *Institute of Nuclear and Physical Engineering, Faculty of Electrical Engineering and Informational Technology, Slovak University of Technology, Ilkovicova 3, 812 19 Bratislava, Slovakia*
[5] *Institute of Medical Chemistry, Biochemistry and Clinical Biochemistry, Faculty of Medicine, Comenius University, Sasinkova 2, 811 08 Bratislava, Slovakia*

Abstract. This work provides complex characterisation of cirrhotic rat liver tissue induced by carbon tetrachloride using biochemical and histopathological analyses, and also presents a novel approach, secondary ion mass spectrometry (SIMS). According to our knowledge, this is the first report that compares these three different approaches in study of liver damage. We observed increased levels of triacylglycerols and total cholesterol in the liver and decreased levels of those parameters in the plasma. Histopathological observations include fat accumulation in the cells and changes in internal configuration of cells such as shift of position of organelles from the centre to the edge. The damage to the rat tissue is additionally determined by SIMS analysis, which characterizes, among other substances, diacylglycerols, cholesterol and fatty acids, such as linoleic and oleic acids. Interestingly, unlike other observed particles, a marked difference in SIMS intensity for diacylglycerol $C_{37}H_{69}O_4$ positive fragment at 575.5 m/u was observed. In fact, there was one order of magnitude difference between intoxicated liver samples and controls and this molecular signal seems to be a potential chemical indicator of the damage. The SIMS images are consistent with histopathological results and they additionally provide information about distribution of chemical compound which is a new potential tool for the liver disease characterisation on molecular level.

Key words: Rat liver — CCl_4 — Biochemical parameters — Histology — SIMS

Abbreviations: ALT, alanine aminotransferase; AST, aspartate aminotransferase; CCl_4, carbon tetrachloride; CYP450, cytochrome P450; HCC, hepatocellular carcinoma; MC, maximum number of detected ions as count *per* pixel; SIMS, secondary ion mass spectrometry; TAG, triacylglycerol; TC, total number of detected ions as count; tChol, total cholesterol; VLDL, very-low-density lipoprotein.

Correspondence to: Jana Muchová, Department of Medical Chemistry, Biochemistry and Clinical Biochemistry, Faculty of Medicine, Comenius University, Sasinkova 2, 811 08 Bratislava, Slovakia
E-mail: jana.muchova@fmed.uniba.sk
* equal contribution

Introduction

Liver disease refers to a wide spectrum of acute conditions caused by various harmful agents. Agents such as viruses, toxins, alcohol and pharmacological compounds as well

as chronic liver diseases might lead to cirrhosis which is a predisposition to hepatocellular carcinoma (HCC) (Burroughs and McNamara 2003). In Europe, approximately 29 million people suffer from the chronic liver conditions and the liver cirrhosis is responsible for approximately 170,000 deaths each year (Blachier et al. 2013). The incidence of HCC in recent decades has increased threefold and the upward trend is expected. Therefore, it is necessary to continue in the intensive research of events leading to cirrhosis, searching for new methods of diagnostics and testing therapeutic potential of new drugs and supplements.

A condition described as cirrhosis results from different mechanisms of liver injury that lead to necroinflammation and fibrogenesis; histologically it is characterised by diffuse nodular regeneration surrounded by dense fibrotic septa with subsequent parenchymal extinction and collapse of liver structures, together causing pronounced distortion of hepatic vascular architecture. This distortion results in increased resistance to portal blood flow and hence in portal hypertension and in hepatic synthetic dysfunction (Tsochatzis et al. 2014). Many conditions leading to cirrhosis are associated with a change in lipid metabolism, for example: alcoholic liver disease, non-alcoholic fatty liver, which is the first stage of non-alcoholic fatty liver disease, which besides simple steatosis includes another stage, which is non-alcoholic steatohepatitis. In industrialised countries, obesity, associated with non-alcoholic steatohepatitis, is becoming a common cause of chronic liver disease leading to cirrhosis, either as the sole cause or in combination with alcohol, hepatitis C, or both (Pinzani et al. 2011).

Secondary ion mass spectrometry (SIMS) is a very sensitive analytical method suitable for chemical characterisation of different materials. A principle of the SIMS method is based on surface bombardment with high energy ions and secondary ions that are emitted in the process are analysed. SIMS is widely used for characterisation of inorganic (Benninghoven 1969; Van Vaeck 2001; Szymczak et al. 2006; Awazu et al. 2008), organic (Benninghoven 1994; Colliver et al. 1997; Mannini et al. 2007) and also biological samples (Nygren et al. 2004; Jones et al. 2007). SIMS combines identification and localisation of different chemical species in the form of mass spectrum and imaging, respectively. The mass spectrum is a function of secondary ion intensity on mass-to-charge ratio, m/u and the chemical imaging is a function of the secondary ion intensity of the specific mass related to the position on the sample surface. The characterisation of biological samples using those two modes is possible due to the development of the clusters of primary ion sources like Au_n^{q+} and Bi_n^{q+}, (n = 1–3, q = 1,2), which allows better lateral and mass resolution (Winograd 2005), compared to conventional atomic ion beams such as Ga^+ and Cs^+. Atomic ion beam penetrates deeply into the sample which results in the breaking of molecular bonds inside the sample. When a cluster ion beam is used, each atom in the cluster retains only a fraction of the initial energy of the ion, thus resulting in a significant reduction in penetration depth of the ion. SIMS can identify the positions of lipids, proteins and DNA directly in a cell or a tissue sample (Altelaar et al. 2006). The localisation of certain molecules within the sample is crucial for understanding the structure of the cells and tissues. Moreover, SIMS can also reveal the cellular response to different substances or various pathological conditions and was successfully used as the diagnostic tool in investigation of lipid-related diseases, such as Duchenne muscular dystrophy (Passarelli and Winograd 2011), non-alcoholic fatty liver disease (Debois et al. 2009), atherosclerosis (Mas et al. 2007), cystic fibrosis (Touboul et al. 2011), cardiac diseases (Aranyosiova et al. 2006), as well as various cancers.

The aim of the presented study was to characterize and compare healthy rat liver tissues with those damaged by carbon tetrachloride (CCl_4) intoxication using SIMS technique. SIMS was used to determine chemical composition and lateral imaging. These were compared with the biochemical and histological/histopathological results, respectively. The liver damage caused by CCl_4 is a model of free radical mediated injury widely used for liver fibrosis and cirrhosis research in experimental animals (Jiang et al. 1992; Uličná et al. 2008; Chávez et al. 2010). According to our knowledge, among many biological studies (animal/human) in which SIMS was used, there are no similar studies of liver tissue intoxication leading to cirrhosis. Hepatic morphological changes are mostly studied by using radiography, computer tomography, magnetic resonance imaging, ultrasonography, nuclear imaging or angiography (Brancatelli et al. 2007). These techniques are widely used in practice and also in biological research, but their results alone are not sufficient to confirm the diagnosis of cirrhosis. The diagnosis in practice is determined using various examination methods and then confirmed by histopathological results obtained from a biopsy sample. In our study, the SIMS spectra and images are consistent with both biochemical parameters and histopathology images.

Materials and Methods

Carbon tetrachloride CCl_4 (Centralchem, Slovak Republic) was diluted in olive oil (VÚLM SK, Slovak Republic) in a 1:2 ratio and was administered *intraperitoneally* (*i.p.*) to the experimental animals. Those animals were fed by the complete diet for laboratory rats and mice such as KKZ-P/M (reg. no 6147).

Wistar male rats (n = 16) were obtained from the Department of Toxicology and Laboratory Animal Breeding at Dobrá Voda, Institute of Experimental Pharmacology and Toxicology, SAS, the approval number SK CH 40004.

The experiment was carried out in accordance with the EU Directive 2010/63/EU and the Slovak Republic Government Regulation establishing requirements for protection of animals used for experimental purposes and other scientific purposes, Z.Z. 23/2009. The protocol was approved by the Local Ethics Committee of Faculty of Medicine Comenius University for animal experiments and the State Veterinary and Food Administration of the Slovak Republic, No. Ro 1766/12-221/3. Rats were housed in cages at a constant temperature of 22 ± 2°C. Their weight was between 330 and 380 g at 5–6 weeks of age. They were subjected to a standard 12 h light/dark cycle and were provided with water and food *ad libitum*. Animals were randomly divided into groups according to the treatment they received: control group (Control) without CCl_4 intake, which was treated only with a vehicle of olive oil; and liver intoxicated group (CCl_4) receiving CCl_4 two times *per* week. Liver intoxication was induced by *i.p.* injection containing solution of CCl_4 in olive oil in amount of 1 ml/kg of body weight (according to Uličná et al. 2003, 2008). The duration of experiment was 10 weeks and then the animals were anesthetised by injection of sodium pentobarbital (*i.p*. 60 mg/kg, 10%). Their livers were surgically excised, rinsed in saline solution, and portions were immediately frozen at −80°C. Preparation of liver homogenate: tissue (1 g) was gently homogenised in 10 ml 0.25 M cold sucrose with 1 mmol/l EDTA (pH 7.4), using a tissue glass Teflon Potter homogenizer 1 time for 25 s. The liver homogenate was used for TAG analyses (commercial diagnostic kit DOT Diagnostics, s.r.o. Prague, Czech Republic, Triglyceridy DST-P). Samples of liver tissue for cholesterol determination were homogenised in a chloroform-methanol mixture (1:1). Total cholesterol in liver homogenate was determined according to Abell et al. (1952). Blood was collected from the abdominal aorta of anaesthetised rats into heparin coated tubes, centrifuged (RT, 1200 × *g*, 10 minutes) to separate plasma from the blood elements. Plasma samples were immediately aliquoted and stored at −80°C until biochemical analysis. Concentrations of total cholesterol (tChol), triacylglycerol (TAG) and activities of alanine aminotransferase (ALT), aspartate aminotransferase (AST) in plasma were determined in a certified laboratory (AlphaMedical Ltd, Slovakia) using an ADVIA 1800 Chemistry System (Siemens Healthcare Diagnostics, Germany).

The experimental data were expressed as the mean ± SEM. Statistical analysis was performed using Student´s *t*-test (IBM SPSS Statistics 24, USA). The limit for statistical significance was set at $p < 0.05$.

Liver samples for histology were fixed in 4% formaldehyde and embedded in paraffin. Liver samples were cut into 4 μm slices. The macrovesicular steatosis was analysed by light microscopy (Microscop Leica DM2000 (Wetzlar, Germany)) in hematoxylin and eosin stained liver slides. The steatotic area was measured by histomorphometry in 10 microscopic fields at 20× magnification using the ImageJ morphometric software v.1.51 (National Institutes of Health, USA) (Abramoff et al. 2004).

The samples for SIMS were prepared in the following way: liver was cut into 40 μm thick slices by using cryomicrotomy (Leika SM 2000 R, Germany) at temperature of –24°C, deposited on glass plate and dried at room temperature. SIMS measurements were performed by using a TOF-SIMS IV (ION-TOF, Germany), a reflectron type of time-of-flight mass spectrometer equipped with a bismuth ion source. The sample was bombarded by pulse focused beam of primary ions (Bi^+) with energy 25 keV. The current of primary ions was 1 pA. The SIMS spectra were measured by scanning over the 100 × 100 μm^2 analysis area with the total primary ion dose density within the static limit of 10^{13} ions *per* square centimeter. Imaging was performed by selecting masses of interest and recording their intensities with respect to the position of the primary ion beam in the observed fields 200 × 200 μm^2 large. Primary ion dose density for images was 10^{12} ions *per* cm^2. The lateral resolution of measured 2D images was about 1 μm. Measurements were performed in positive and negative polarities. For evaluation of measurement was used software SurfaceLab 6 (ION TOF GmbH, Muenster, Germany).

Results and Discussion

As expected, 10-weeks of *i.p*. administration of CCl_4 to experimental animals induced pathological changes in the rat organism, blood and liver. Reduction in the rate of body weight increase and increase in the ratio of liver weight to body weight expressed as hepatosomatic index HI, confirmed severe liver damage. Biochemical parameters ALT, AST, TAG, tChol were determined since those parameters are part of a routine examination in case of liver injury (cirrhosis). Although they are not specific, they contribute to assessing the liver functionality and they are necessary to determine the status of liver. There is no single specific diagnostic marker of cirrhosis, in practice the diagnosis is always determined using multiple parameters (biochemistry results + physical examination + imaging techniques/biopsy). In this work, we have selected those biochemical/histological parameters that characterize the tissue conditions and at the same time they correspond to the parameters provided by SIMS analysis.

Increased activities of ALT and AST in plasma (Tab. 1) indicate disruption of the plasma membrane of hepatocytes primarily as a result of lipid peroxidation caused by $CCl_3^{\bullet}$ radical formed during CCl_4 metabolism by the cytochrome oxidase system (Weber et al. 2003). The increased concentrations of TAG and tChol were observed in the liver (Tab. 1), in accordance with Uličná et al. (2008), while in

Table 1. Biochemical parameters in plasma and liver and histological parameter – steatosis in liver of Control and CCl_4 intoxicated rats

	Control	CCl_4
Biochemical parameters in plasma		
ALT (μkat/l)	0.40 ± 0.03	7.28 ± 1.18**
AST (μkat/l)	1.19 ± 0.09	7.19 ± 1.12**
tChol (mmol/l)	1.37 ± 0.07	0.80 ± 0.16**
TAG (mmol/l)	1.30 ± 0.15	0.50 ± 0.03**
Biochemical parameters in liver		
tChol (mmol/kg)	4.34 ± 0.18	10.81 ± 0.74**
TAG (mmol/kg)	13.85 ± 1.47	63.05 ± 10.56**
Histological parameter in liver		
Steatosis (%)	100 ± 15.57	584.6 ± 64.16***

Data are presented as the mean ± SEM; ** $p < 0.01$, *** $p < 0.001$ *versus* Control group.

plasma the levels of these lipids were decreased (Tab. 1). According to the review article by Weber et al. (2003) these changes are mainly caused by impaired transport systems of the liver, which is observed in CCl_4 model. The accumulation of fat is associated with disrupted protein synthesis in the cells resulting in the lack of apolipoproteins required for the transport of very-low-density lipoprotein (VLDL), that are used for transport of triacylglycerols from the liver into the blood stream. Elevation of AST activity indicates partially damaged mitochondria observed also by other authors working with CCl_4 model (Krähenbühl et al. 1990) and this mitochondrial damage may lead to impaired β-oxidation of fatty acids. The reduction in β-oxidation induced by CCl_4 was confirmed in Hepatocyte cultures also by Boll et al. (2001) and is explained by the inactivation of cytochrome P-450 *via* AMP-activated protein kinase signalling pathway. Reduced degradation of fatty acids, increased synthesis of TAG and disrupted transport observed in CCl_4 model could together lead to the accumulation of TAG in the liver.

Histopathological measurements confirmed development of steatosis and fibrosis in rat liver after 10-weeks of CCl_4 administration. The toxic damage of liver tissue caused by CCl_4 is most prevalent in those hepatocytes which contain high activities of cytochrome enzyme system, especially CYP450 2E1 (Delaney 2006). As mentioned above, CCl_4 is metabolised by this system into highly reactive and highly toxic radical $CCl_3^{\bullet}$ that quickly reacts with nearby molecules of lipids, proteins, and nucleic acids. Since hepatocytes with high activity of this enzyme reside in the vicinity of a terminal branch of hepatic vein (*v. centralis*, Fig. 1(h), Fig. 2(g)), it is this pericentral zone that is damaged the most and this is the spot where can be preferentially by acute intoxication observed necrosis of hepatocytes. Free radicals damage membranes which impair their integrity and function, and leads to increased mass of lipids stored in the cells. The lipid droplets change the inner arrangement of hepatocytes in a way that cell organelles are pushed to the side of the hepatocyte Fig. 2(c) and hepatocytes can be enlarged. Compared to controls (Fig. 1), carbon tetrachloride administration (Fig. 2) caused the development of liver steatofibrosis characterised by lipid accumulation in hepatocytes in the form of microvesicular Fig. 2(a), and macrovesicular Fig. 2(b) steatosis, with the parallel nuclear crowding to the side of the cell Fig. 2(c). The portal spaces are extended, forming the fibrous bridges between themselves Fig. 2(d), with the formation of liver pseudolobules Fig. 2(e) and with asymmetrical abnormal location of central veins Fig. 2(g). No changes were observed in control animals with the physiological formation of hepatocytic plates Fig. 1(f) and central veins, as shown in Fig. 1(h). Quantification of histology is presented in Table 1.

SIMS technique provides information about the chemical composition of liver slides surface in the form of mass spectra and two-dimensional images. The mass spectra reveal atoms, molecules, and molecular fragments of the tissue and the two-dimensional images demonstrate the lateral distribution of selected biologically relevant chemical species on the tissue surface (Piwowar and Winograd 2013). The main goal of this work was to chemically differentiate between healthy (Control) and intoxicated liver tissues (CCl_4). Characteristic masses identified in the healthy and intoxicated liver tissues are presented in Tab. 2 in positive and negative polarities. Note, that there is no significant qualitative difference between chemical composition of healthy and cirrhotic liver tissue. All peaks shown in the Tab. 2 were identified in mass spectra of all samples.

The main differences between the healthy and intoxicated tissues are given by comparison of lipids content as shown in Tab. 3. Table 3 provides selected characteristic mass peaks of healthy and intoxicated tissues and also their approximate ratio. Note, that SIMS intensities are normalised to total ion intensity which provides quantitative comparison of the samples. This normalisation approach is a standard for the relative quantification, since the absolute quantification of SIMS is very limited. In other words, higher SIMS intensity does not represent higher concentration when different species are compared. The intensity of iron species with mass of 55.9 represents a reference, assuming that the Fe concentration should remain constant and in fact we observed that the Fe intensity ratio between healthy and intoxicated tissues was approximately 1. Interestingly, the vitamin E fragment with mass of 430.4 m/u has also the ratio of 1. The phospholipid fragment with the mass of 184.1 m/u and in case of fatty acids content, represented by

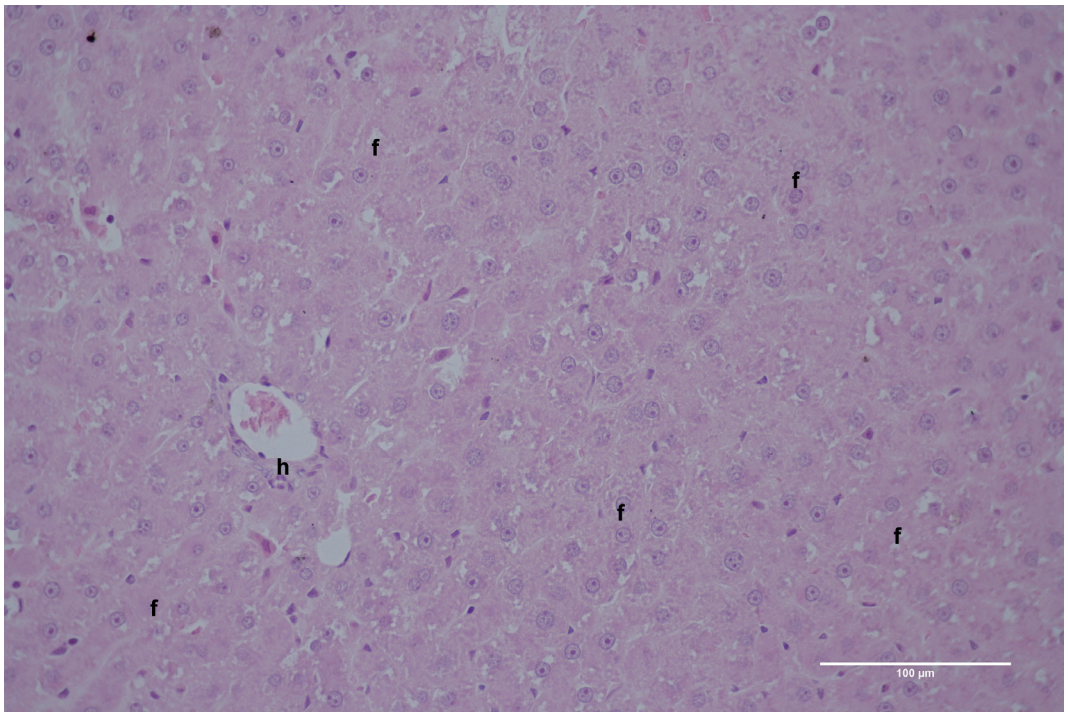

Figure 1. Control group of rats (Control): physiological formation of hepatocytic plates (f) and central veins (h). The scale in the figure represents 100 µm.

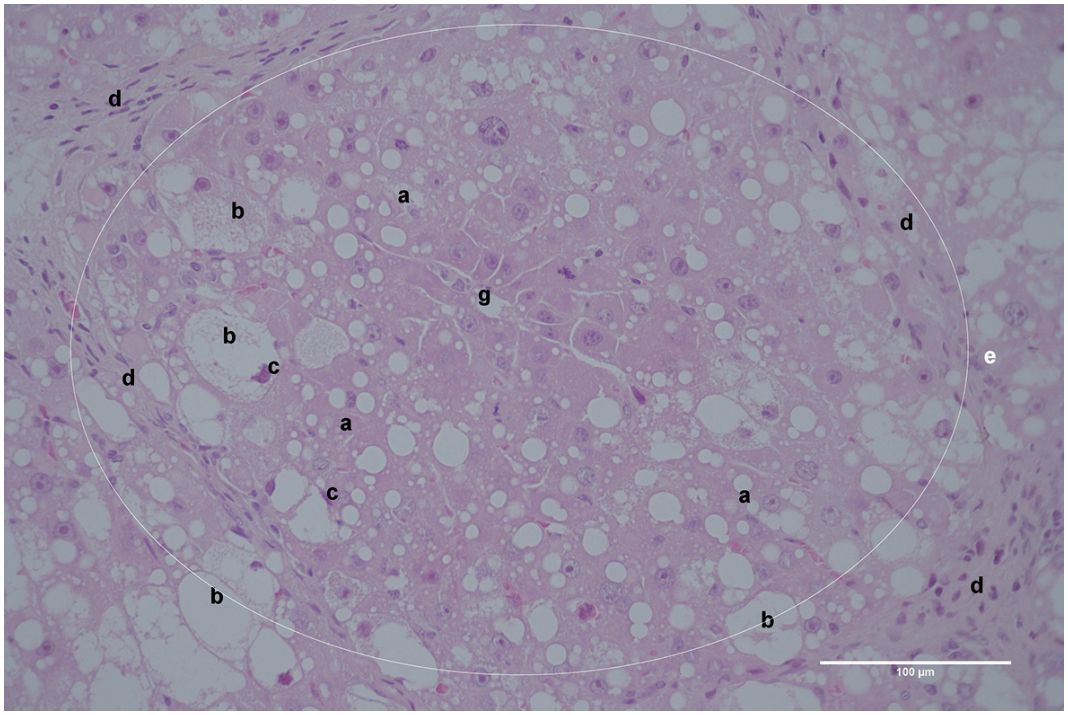

Figure 2. CCl_4-intoxicated group of rats (CCl_4): microvesicular (a) and macrovesicular (b) steatosis, with the parallel nuclear crowding to the side of the cell (c), fibrous bridges (d), formation of liver pseudolobules (e), asymmetrical abnormal location of central veins (g). The scale in the figure represents 100 µm.

Table 2. Mass peak assignments of rat liver tissue (healthy/damaged by CCl_4) in positive and negative polarities

m/u	Fragment	Origin
Positive ions		
	$C_xH_y^+$	Carbohydrates
30	CH_4N^+	Glycine
44	$C_2H_6N^+$	Alanine
70	$C_4H_8N^+$	Proline
84.1	$C_5H_{10}N^+$	Lysine
86.1	$C_5H_{12}N^+$	Leucine
166.1	$C_5H_{12}NPO_3^+$	Phospholipids
184.1	$C_5H_{15}NPO_4^+$	Phospholipids
224.1	$C_8H_{19}NPO_4^+$	Phospholipids
369.4	$C_{27}H_{45}^+$	Cholesterol
385.4	$C_{27}H_{45}O^+$	Cholesterol
430.4	$C_{29}H_{50}O_2^+$	Vitamin E
523.5	$C_{33}H_{63}O_4^+$	Diacylglycerol
551.5	$C_{35}H_{67}O_4^+$	Diacylglycerol
575.5	$C_{37}H_{69}O_4^+$	Diacylglycerol
603.6	$C_{39}H_{71}O_4^+$	Diacylglycerol
Negative ions		
	$C_xH_y^-$	Carbohydrates
17	OH^-	Amino Acids
26	CN^-	Peptides
33	SH^-	Amino Acids
42	CNO^-	Peptides
47, 63, 79, 95	PO_x^- x= 1 – 4	Phospholipids
255.2	$C_{16}H_{31}O_2^-$(16:0)*	Palmitic acid
279.2	$C_{18}H_{31}O_2^-$(18:2)*	Linoleic acid
281.2	$C_{18}H_{33}O_2^-$(18:1)*	Oleic acid
283.2	$C_{18}H_{35}O_2^-$(18:0)*	Stearic acid

* Number of C atoms to double bonds.

linoleic acid with mass 279.2 m/u and oleic acid with mass 281.2 m/u, their ratios were approximately 2. The intensity of cholesterol peak with mass of 369.2 m/u was approximately 3 times higher in the damaged tissue compared to the healthy tissue. The magnitude of difference in case of cholesterol implies, that this parameter might be used to differentiate between healthy and intoxicated tissue. Interestingly, there was almost one order of magnitude difference between the healthy and cirrhotic liver, when the intensities of fragments which belong to diacylglycerols with mass of 551.5 and 575.5 m/u were compared. The diacylglycerols content is higher in intoxicated tissue and this molecular signal might be used as a chemical indicator of the damaged tissue intoxicated with CCl_4.

Liver cirrhosis is a result of a diffuse process terminated in the complete disorganisation of the liver structure. Localisation of biomolecules in tissue samples is important to understand the chemical and also morphological changes in healthy and diseased tissue. The SIMS technique is an excellent way to map chemical morphology. The SIMS images, shown in Fig. 3, represent the two-dimensional distribution of selected molecular fragments typical for the liver tissue listed in Tab. 2 and Tab. 3. The images were measured on an area 200 × 200 μm^2. The intensity of the yellow colour in images represents the abundance of selected secondary ions in measured area (colour scale is included in the images). More intensive colour means higher intensity of emitted secondary ions. The dark colour means low or no emission of selected secondary ions. The numbers below each image denote the maximum number of detected ions as maximum count (MC) *per* pixel and the total number of detected ions as total count (TC). For the analysis following species of interest in negative polarity were selected: Cl^- – sum of isotopes $^{35}Cl^-$ (34.9 m/u) and $^{37}Cl^-$ (36.9 m/u), phospholipids – sum of PO_3^- (78.9), $PO_4H_2^-$ (97 m/u) and $C_{11}H_{14}PO_4^-$ (241.1 m/u), and fatty acids – sum of $C_{16}H_{31}O_2^-$ (255.2 m/u), $C_{18}H_{31}O_2^-$ (279.2 m/u), $C_{18}H_{33}O_2^-$ (281.2 m/u), $C_{18}H_{35}O_2^-$ (283.2 m/u). The total ion image represents the distribution of all secondary ions detected during SIMS analysis in selected polarity. In the upper row of Fig. 3, the distributions of chlorine species, phospholipids, fatty acids and total ions in control tissue are shown. The first image represents the sum of secondary ions intensities for chlorine isotopes $^{35}Cl^-$ and $^{37}Cl^-$. The low intensity, reflects the physiological quantity of Cl^-, corresponding to NaCl, the image is without contours and homogeneous and correspond to total ion distribution. Second image in the row represents the sum of secondary ions for phospholipids fragments, as shown in the Table 2. The intensity is higher as for chlorine species and distribution is homogeneous and without any special features. Third image in the row represents the sum of fatty acids fragments, as shown in the Table 2. The intensity is lower than for phospholipids fragments but the distribution is also homogeneous.

In the lower row of Fig. 3, the distribution of the same species is shown for the damaged tissue. The chlorine species have low intensities also in the damaged tissue despite the intoxication by CCl_4 and their contours correspond to total ion distributions as in the first row. The comparable SIMS intensities of chlorine species in the control and the intoxicated tissue could be explained by degradation of CCl_4 into chloride anions which are not accumulated in the cell and can eventually be excreted. Second image represents the phospholipid fragments distribution with some heterogeneity features. Also the third image representing the fatty acids distribution shows some heterogeneous contours contrary to the distributions of control tissue.

From the viewpoint of SIMS comparison with other used methods there was found, that the concentration of

Table 3. SIMS intensities of selected species of healthy and CCl_4 intoxicated rat liver tissues and their approximate ratio

	Mass (Species)							
	55.9 (Fe^+)	184.1 ($C_5H_{15}NPO_4^+$)	369.2 ($C_{27}H_{45}^+$)	430.4 ($C_{29}H_{50}O_2^+$)	551.5 ($C_{35}H_{67}O_4^+$)	575.5 ($C_{37}H_{69}O_4^+$)	279.2 ($C_{18}H_{31}O_2^-$)	281.2 ($C_{18}H_{33}O_2^-$)
Control ($\times 10^{-5}$)	1.23	810.00	6.69	17.40	0.57	1.16	3.67	4.23
CCl_4 ($\times 10^{-5}$)	1.14	1560.00	18.00	12.20	2.95	12.30	8.04	10.30
approx. ratio	1	2	3	1	5	10	2	2

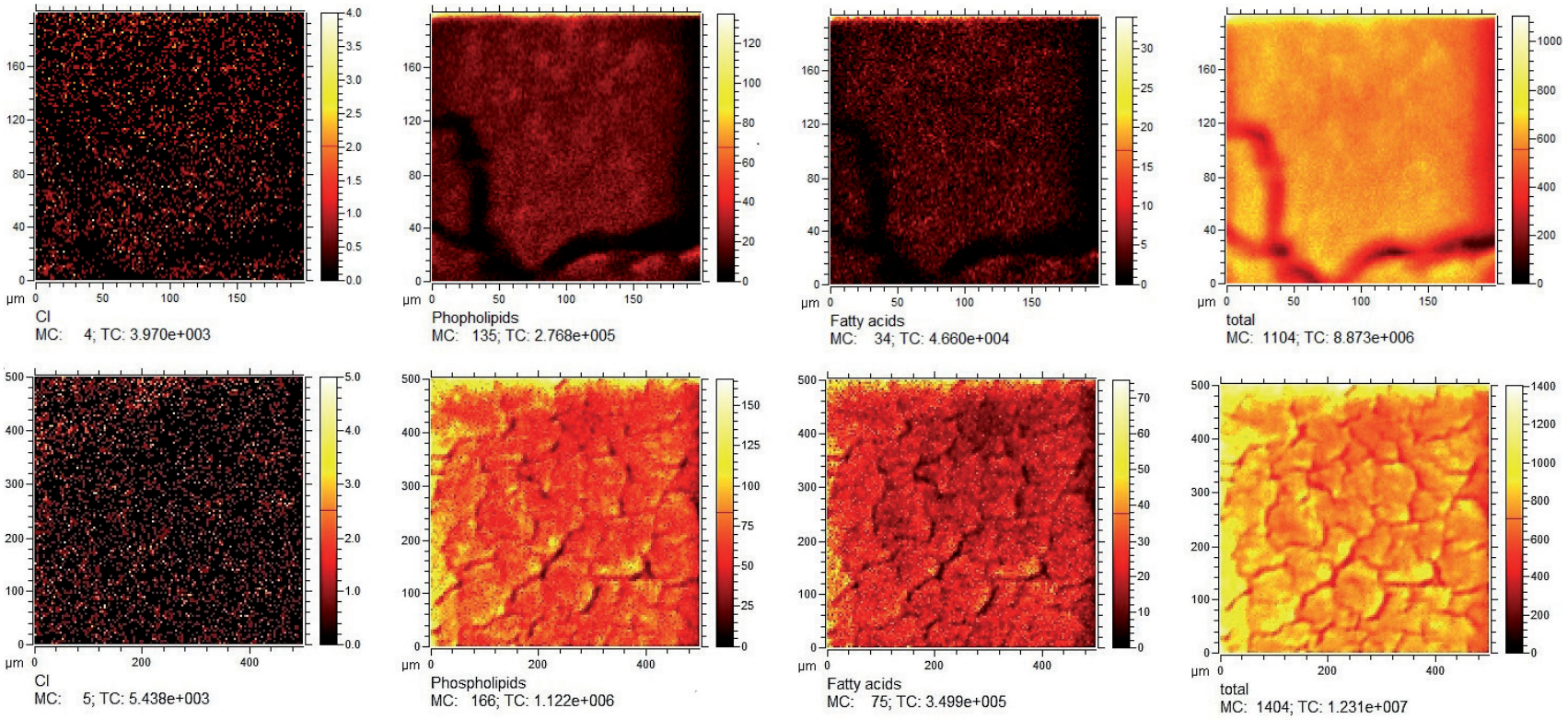

Figure 3. Two dimensional SIMS images as chemical distributions of selected species on rat liver tissues; the control tissue in an upper row and the CCl_4-intoxicated tissue in a lower row. The numbers below each image denote the maximum number of detected ions as maximum count (MC) *per* pixel and the total number of detected ions as total count (TC).

liver acylglycerols determined by biochemical methods was statistically significantly increased by factor 4.5 (Tab. 1), histology recorded a statistically significant increase in fat area by factor 5.8 (Tab. 1) and SIMS method shows approximately one order increase in intensities of fragments which originate from diacylglycerols (factor 10 in Tab. 3). When comparing biochemistry and SIMS, both methods found the increased cholesterol in the liver (tChol increase by factor 2.5 (Tab. 1), SIMS by factor 3 (Tab. 3)), but in both methods this increase was not as significant as the increase in acylglycerols. These results represent just a rough comparison due to the diametrical difference of techniques.

Conclusions

All three used methods – biochemical methods, histopathological methods and mass spectrometry – showed a significant change in the composition and/or structure of rat liver tissue after prolonged exposure to CCl_4. The significant changes in lipid metabolism and their distribution between liver tissue and plasma from a biochemical point of view were observed as the increased TAG and tChol levels in the liver homogenate with simultaneous decline of these parameters in the plasma. There is a consistency between biochemical and SIMS results, both of which show a multiple increase in glycerol esters in the liver compared to the rise in cholesterol in this tissue. The histopathological measurements in 10 microscopic fields confirmed the accumulation of fat in hepatocytes, as well as changes in its distribution – the increased amount of fats distorts the internal configuration of cells, and suppresses of some structures from the centre to the edge of the cell. In addition, the specification of liver lipids by SIMS facilitates understanding of ongoing steatotic processes. SIMS provides the most detailed information – on the molecular level, thus enabling its utilisation in this field of study. Despite of different approaches of all three mentioned techniques, the obtained results are in a good agreement and they complement each other. Biochemical methods provide the information about the liver tissue in general while histology/histopathology and SIMS provide map of a certain (damaged) area. To achieve the most complete and detailed information of the real tissue in the research field, combination of several techniques with different characteristics is essential.

Results of our basic research are a rare view of still-evolving SIMS technology that has a high potential in study of tissue damage at the molecular level.

Acknowledgements. Presented work was supported by VEGA grant 1/1133/11, APVV-15-0201 and Mind and Health, civil association.

References

Abell LL, Levy BB, Brodie BB, Kendall FE (1952): A simplified method for the estimation of total cholesterol in serum and demonstration of its specificity. J. Biol. Chem. **195,** 357–366

Abramoff MD, Magelhaes PJ, Ram SJ (2004): Image processing with image. J. Biophotonics International **11,** 36–42

Altelaar AFM, Klinkert I, Jalink K, de Lange RPJ, Adan RAH, Heeren RMA, Piersma SR (2006): Gold-enhanced biomolecular surface imaging of cells and tissue by SIMS and MALDI mass spectrometry. Anal. Chem. **78,** 734–742 https://doi.org/10.1021/ac0513111

Aranyosiova M, Chorvatova A, Chorvat D, Jr, Biro C, Velic D (2006): Analysis of cardiac tissue by gold cluster ion bombardment. App. Surf. Sci. **252,** 6782–6785 https://doi.org/10.1016/j.apsusc.2006.02.182

Awazu K, Fujimaki M, Rockstuhl C, Tominaga J, Murakami H, Ohki Y, Yoshida N, Watanable T (2008): A plasmonic photocatalyst consisting of silver nanoparticles embedded in titanium dioxide. J. Am. Chem. Soc. **130,** 1676–1680 https://doi.org/10.1021/ja076503n

Benninghoven A (1969): Analysis of submonolayers on silver by negative secondary ion emission. Phys. Status. Solidi. **34,** 169–171 https://doi.org/10.1002/pssb.19690340267

Benninghoven A (1994): Chemical analysis of inorganic and organic surfaces and thin films by static time-of-flight secondary ion mass spectrometry (TOF-SIMS). Angew. Chem. Int. Ed. **33,** 1023–1043 https://doi.org/10.1002/anie.199410231

Blachier M, Leleu H, Peck-Radosavljevic M, Valla DC, Roudot-Thoraval F (2013): The burden of liver disease in Europe: A review of available epidemiological data. J. Hepatol. **58,** 593–608 https://doi.org/10.1016/j.jhep.2012.12.005

Boll M, Weber LW, Becker E, Stampfl A (2001): Pathogenesis of carbon tetrachloride-induced hepatocyte injury bioactivation of CC14 by cytochrome P450 and effects on lipid homeostasis. Z. Naturforsch. **56c,** 111–121 https://doi.org/10.1515/znc-2001-1-218

Brancatelli G, Federle MP, Ambrosini R, Lagalla R, Carriero A, Midiri M, Vilgrain V (2007): Cirrhosis: CT and MR imaging evaluation. Eur. J. Radiol. **61,** 57–69 https://doi.org/10.1016/j.ejrad.2006.11.003

Burroughs A, McNamara D (2003): Liver disease in Europe. Aliment. Pharmacol. Ther. **18** (Suppl. 3), 54–59 https://doi.org/10.1046/j.0953-0673.2003.01729.x

Chávez E, Segovia J, Shibayama M, Tsutsumi V, Vergara P, Castro-Sánchez L, Pérez Salazar E, Moreno MG, Muriel P (2010): Antifibrotic and fibrolytic properties of celecoxib in liver damage induced by carbon tetrachloride in the rat. Liver Int. **30,** 969–978 https://doi.org/10.1111/j.1478-3231.2010.02256.x

Colliver TL, Brummel CL, Pacholski ML, Swanek FD, Ewing AG, Winograd N (1997): Atomic and molecular imaging at the single-cell level with TOF-SIMS. Anal. Chem. **69,** 2225–2231 https://doi.org/10.1021/ac9701748

Debois D, Bralet MP, Le Naour F, Brunnelle A, Laprévote O (2009): In situ lipidomic analysis of nonalcoholic fatty liver by cluster TOF-SIMS imaging. Anal. Chem. **81,** 2823–2831

https://doi.org/10.1021/ac900045m
Delaney KA (2006): Hepatic principles In: Goldfrank's Toxicologic Emergencies. (Eds. Flomenbaum N, Goldfrank L, Hoffman R, Howland MA, Lewin N, Nelson L), pp. 412–420, 8th edition, McGraw-Hill Professional, ISBN: 978-0071437639
Jiang Z, You DY, Chen X, Wu J (1992): Monitoring of serum markers for fibrosis during CCl4-induced liver damage. Effects of anti-fibrotic agents. J. Hepatol. **16,** 282–289 https://doi.org/10.1016/S0168-8278(05)80658-0
Jones EA, Lockyer NP, Vickerman JC (2007): Mass spectral analysis and imaging of tissue by ToF-SIMS – The role of buckminsterfullerene, C 60+, primary ions. Int. J. Mass. Spec. **260,** 146–157 https://doi.org/10.1016/j.ijms.2006.09.015
Krähenbühl S, Reichen J, Zimmermann A, Gehr P, Stucki J (1990): Mitochondrial structure and function in CCl4 induced cirrhosis in the rat. Hepatology **12,** 526–532 https://doi.org/10.1002/hep.1840120313
Mannini M, Sorace L, Gorini L, Piras FM, Caneschi A, Magnani A, Menichetti S, Gatteschi D (2007): Self-assembled organic radicals on Au (111) surfaces: a combined ToF-SIMS, STM, and ESR study. Langmuir **23,** 2389–2397 https://doi.org/10.1021/la062028f
Mas S, Touboul D, Brunelle A, Aragoncillo P, Egido J, Laprévote O, Vivanco F (2007): Lipid cartography of atherosclerotic plaque by cluster-TOF-SIMS imaging. Analyst **132,** 24–26 https://doi.org/10.1039/B614619H
Nygren H, Malmberg P, Kriegeskotte C, Arlinghaus HF (2004): Bioimaging TOF-SIMS: localization of cholesterol in rat kidney sections. FEBS Lett. **566,** 291–293 https://doi.org/10.1016/j.febslet.2004.04.052
Passarelli MK, Winograd N (2011): Lipid imaging with time-of-flight secondary ion mass spectrometry (ToF-SIMS). Biochim. Biophys. Acta **1811,** 976–990 https://doi.org/10.1016/j.bbalip.2011.05.007
Pinzani M, Rosselli M, Zuckermann M (2011): Liver cirrhosis. Best Practice & Research Clinical Gastroenterology **25,** 281–290 https://doi.org/10.1016/j.bpg.2011.02.009
Piwowar AM, Winograd N (2013): Application of SIMS to study of biological systems. In: Materials Analysis by Mass Spectrometry. (Eds. Vickerman JC, Briggs D), pp. 553–582, TOF-SIMS: IM Publications LLP, UK, ISBN 978-1-906715-17-5,
Szymczak W, Menzel N, Kreyling WG, Wittmaack K (2006): Tof-sims characterisation of spark-generated nanoparticles made from Pairs of Ir–Ir and Ir–C electrodes. Int. J. Mass Spec. **254,** 70–84 https://doi.org/10.1016/j.ijms.2006.05.010
Touboul D, Laprévote O, Brunelle A (2011): Micrometric molecular histology of lipids by mass spectrometry imaging. Curr. Opin. Chem. Biol. **15,** 725–732 https://doi.org/10.1016/j.cbpa.2011.04.017
Tsochatzis EA, Bosch J, Burroughs AK (2014): Liver cirrhosis. Lancet **383,** 1749–1761 https://doi.org/10.1016/S0140-6736(14)60121-5
Uličná O, Greksák M, Vančová O, Zlatoš L, Galbavý P, Božek P, Nakano M (2003): Hepatoprotective effect of rooibos tea (Aspalathus linearis) on CCl4-induced liver damage in rats. Physiol. Res. **52,** 461–466
Uličná O, Vančová O, Waczulíková I, Božek P, Janega P, Babál P, Lišková S, Greksák M (2008): Does rooibos tea (Aspalathus linearis) support regeneration of rat liver after intoxication by carbon tetrachloride? Gen. Physiol. Biophys. **27,** 179–186
Van Vaeck L (2001): Molecular speciation analysis of inorganic compounds. In: Surface Analysis by Mass Spectrometry. (Eds. Vickermann JC, Briggs D), IM Publications, Surface Spectra Ltd, UK, ISBN 978-1-901019-03-2
Weber LW, Boll M, Stampfl A (2003): Hepatotoxicity and mechanism of action of haloalkanes: carbon tetrachloride as a toxicological model. Crit. Rev. Toxicol. **33,** 105–136 https://doi.org/10.1080/713611034
Winograd N (2005): The magic of cluster SIMS. Anal. Chem. **77,** 142–149 https://doi.org/10.1021/ac053355f

Received: January 11, 2018
Final version accepted: March 20, 2018